Spectrochimica Acta Part A 81 (2011) 519–528

Contents lists available at ScienceDirect

Spectrochimica Acta Part A: Molecular and Biomolecular Spectroscopy

journal homepage: www.elsevier.com/locate/saa

Elaborated ^{1}H NMR study for the ligitional behavior of two thiosemicarbazide derivatives towards some heavy metals (Sn(II), Sb(III), Pb(II) and Bi(III)), thermal, antibacterial and antifungal studies

Nashwa M. El-Metwaly[a,b], Moamen S. Refat[c,d,*]

[a] Department of Chemistry, Faculty of Science, Mansoura University, Egypt
[b] Department of Chemistry, Faculty of Education of Girls, King Khaled University, Saudi Arabia
[c] Department of Chemistry, Faculty of Science, Port Said University, Port Said, Egypt
[d] Department of Chemistry, Faculty of Science, Taif University, 888 Taif, Saudi Arabia

ARTICLE INFO

Article history:
Received 6 April 2011
Received in revised form 14 June 2011
Accepted 19 June 2011

Keywords:
Thiosemicarbazide
^{1}H NMR
Heavy metals
Thermal

ABSTRACT

A new series of heavy metal complexes are prepared. Sn(II), Sb(III), Pb(II) and Bi(III) are the metal ions used in complexation with two thiosemicarbazide ligands. The IR and ^{1}H NMR spectra of the free ligands display their presence in thiole–thione forms coincide with each other. The IR spectra of the complexes support the presence of 2:2 molar ratio (M:HL) with HL^1 ligand and 1:1 beside 1:2 with HL^2. The ligand coordinates as bi molecules in some complexes and displays two tautomer forms at the same complex molecule ^{1}H NMR spectra of Sn(II) and Sb(III) complexes were done and comes coincide with IR data. The electronic spectral analysis displays a lower shift appearance in $n \rightarrow \pi^*$ charge transfer band in most isolated complexes. As well as, a new band is shinned in visible region with Sb(III), Bi(III) complexes and Sn(II)–HL^2. This band is pointed to its use in spectrophotometric analysis for these metal ions. The TG analysis for all isolated compounds was briefly discussed. The molecular modeling parameters support the stability of thiole form of the free ligands in comparing with their thiones by a small difference. The antibacterial and antifungal activities were studied against some organisms and reveal the priority of most investigated complexes.

1. Introduction

Coordination chemistry of thiosemicarbazides has been a subject of enthusiastic research since they show a wide range of biological properties, especially those derived from heterocyclic aldehydes or ketones. Thiosemicarbazides are versatile ligands having p-delocalization of charge and configurational flexibility of the molecular chain that can give rise to a great variety of coordination modes owing to the interest they generate through a variety of biological properties ranging from anticancer, antitumor, antifungal antibacterial, antimalarial, antifilarial, antiviral and anti-HIV activities [1]. Thiosemicarbazones as well as thiosemicarbazides and their metal complexes have been extensively studied [2,3]. Reports on N(4)-substituted thiosemicarbazides have concluded that the biological activity depends on the parent aldehyde or ketone, the presence of a bulky group at the terminal nitrogen and the presence of an additional potential bonding site [4,5]. They also contain N=C–C=N structure unit, which displays a strong chelating ability through the electron delocalization, which associated with extended conjugation, that may affect the nature of the complex formed. They can yield mono or polynuclear complexes some of which are biologically relevant [6]. In continuation of our investigation on the complexing properties of N(4)-substituted thiosemicarbazides we synthesized the ligands (HL^1) and (HL^2). The first raw transition metal complexes were reported [7,8] for the two ligands under investigation. This work aimed to the preparation of some heavy metal complexes, which is relatively rare with thiosemicarbazides ligands. Here we report the synthesis, structural and spectral characterization of 8 complexes. The biological investigation (antibacterial and antifungal) for all isolated complexes was done in comparing with their relative ligands towards some essential organisms.

2. Experimental

2.1. Reagents

Aldehydes (naphthaldehyde and 2-anisaldehyde) used and thiosemicarbazide was obtained from Fluka. All chemicals used

* Corresponding author at: Department of Chemistry, Faculty of Science, Taif University, Saudi Arabia. Tel.: +966 561926288.
E-mail address: msrefat@yahoo.com (M.S. Refat).

1386-1425/$ – see front matter © 2011 Elsevier B.V. All rights reserved.
doi:10.1016/j.saa.2011.06.045

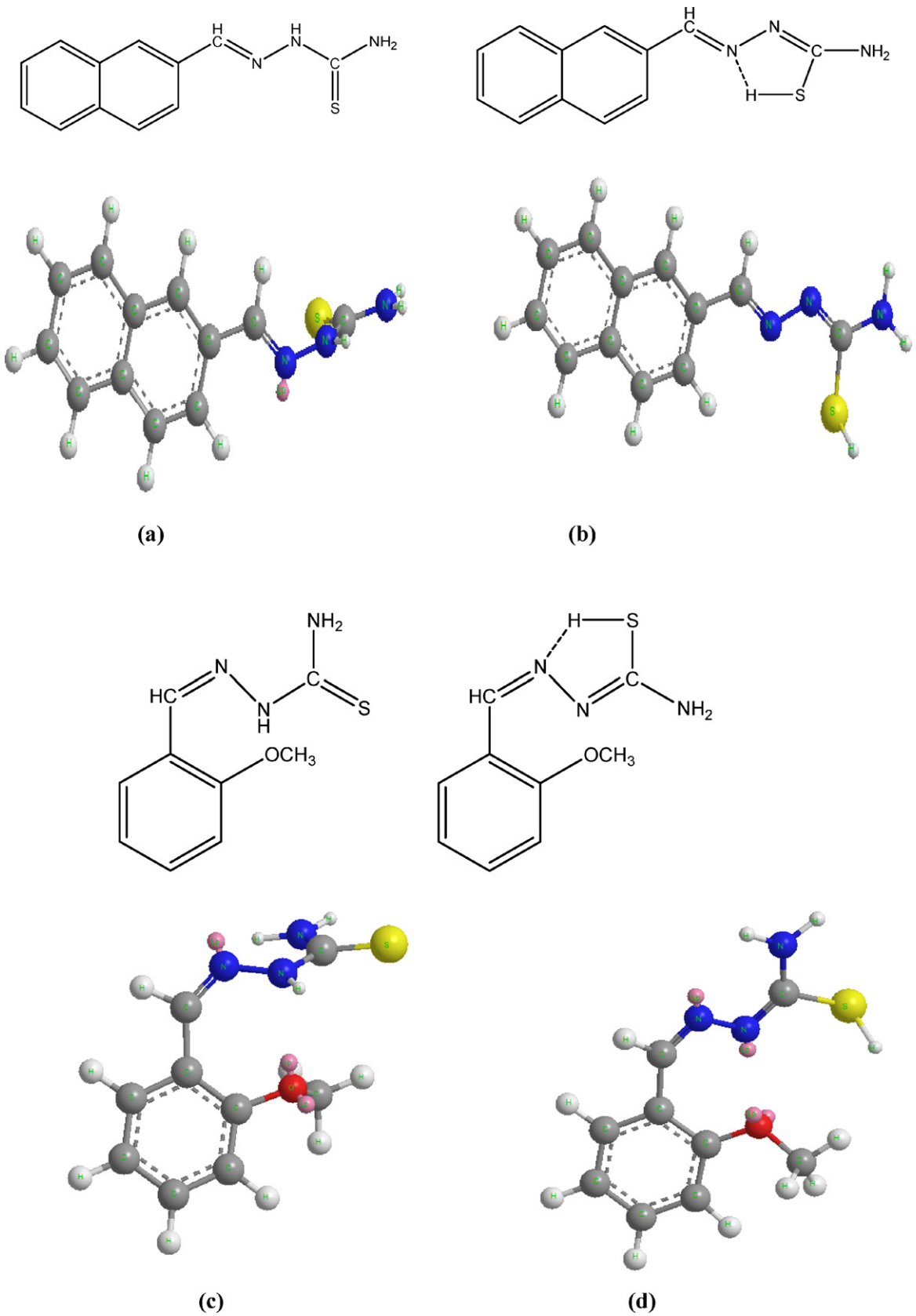

Fig. 1. 1-(Naphthalene-2-ylmethylene) thiosemicarbazide (HL^1) (a, b) (thione–thiole forms), 1-(2-metoxybenzylidene) thiosemicarbazide (HL^2), (c, d) (thione–thiole forms).

Table 1
Analytical and physical data for thiosemicarbazides (HL^1 and HL^2) and their metal complexes.

Compound Empirical formula (M. Wt.)	Color	Λ_m (Ω^{-1} cm^{-1} mol^{-1})	Elemental analysis (%) Found (Calcd.)				
			C	H	N	M	Cl
(1) HL^1 $[C_{12}H_{11}N_3S]$ (229.31)	Light Cream	–	62.85 (62.85)	4.78 (4.84)	18.3 (18.32)	–	–
(2) $[Sn_2Cl_3(C_{12}H_{11}N_3S)_2]Cl{\cdot}4H_2O$ (909.9)	Cream	60.2	31.71 (31.68)	3.35 (3.32)	9.22 (9.24)	26.11 (26.09)	15.61 (15.58)
(3) $[Sb_2Cl_5(C_{12}H_{11}N_3S)_2]Cl{\cdot}4H_2O$ (986.89)	Orange	55.3	29.20 (29.21)	3.11 (3.06)	8.51 (8.52)	24.65 (24.67)	21.54 (21.55)
(4) $[Pb_2(NO_3)_3(C_{12}H_{11}N_3S)_2](NO_3){\cdot}2H_2O$ (1157.06)	Yellow	53.4	24.87 (24.91)	2.26 (2.26)	–	35.80 (35.81)	–
(5) $[Bi_2Cl_5(C_{12}H_{11}N_3S)_2]Cl{\cdot}2H_2O$ (1125.32)	Yellow	55.6	25.60 (25.62)	2.31 (2.33)	7.47 (7.45)	37.10 (37.14)	18.91 (18.90)
(6) HL^2 $[C_9H_{11}N_3SO]$ (209.27) $m/z = 209$	White	–	51.65 (51.66)	5.27 (5.29)	20.1 (20.08)	–	–
(7) $[SnCl_2(C_9H_{11}N_3SO)H_2O]$ (416.9)	Orange	15.1	25.92 (25.93)	3.12 (3.14)	9.89 (10.08)	28.5 (28.47)	17.1 (17.01)
(8) $[SbCl_3(C_9H_{11}N_3SO)_2]H_2O$ (664.66)	Orange	–	32.51 (32.53)	3.56 (3.64)	6.29 (6.32)	18.3 (18.32)	15.98 (16.00)
(9) $[Pb(NO_3)(C_9H_{11}N_3SO)_2]$ (687.74)	White	–	31.51 (31.43)	3.20 (3.22)	–	30.1 (30.13)	–
(10) $[BiCl_3(C_9H_{11}N_3SO)_2H_2O]H_2O$ (560.64)	Orange	–	19.19 (19.28)	2.68 (2.69)	7.47 (7.49)	37.18 (37.27)	18.95 (18.97)

for the study were of analytically reagent grade and used without previous purification as $SnCl_2{\cdot}2H_2O$, $SbCl_3$, $Pb(NO_3)_2$ and $BiCl_3$ compounds, which represents the metal ions in concern for the complexation.

2.2. Synthesis of ligands

The ligands, 1-(naphthalene-2-ylmethylene) thiosemicarbazide (HL^1) (Fig. 1) and 1-(2-methoxybenzylidene) thiosemicarbazide (HL^2) (Fig. 1) were obtained by a general procedure reported [7,8]. This is by reaction of thiosemicarbazide and each aldehyde in 1:1 molar ratio in ethanol–water solution.

2.3. Synthesis of complexes

2.3.1. Synthesis of MHL^1 complexes

To a solution of the respective ligand (2 mmol) in a hot methanol (25 ml) was added metal chloride or nitrate (1 mmol), and the resulting solution was heated under reflux for 2 h. The complexes formed were filtered, washed thoroughly with ethanol and then ether and dried in vacuum over $CaCl_2$.

2.3.2. Synthesis of MHL^2 complexes

To a solution of respective ligand HL^2 (2 mmol) in a hot methanol (25 ml) was added metal chloride or nitrate (1 mmol), and the resulting solution was heated and the complexes were suddenly precipitated during a reflux for 0.5 h only. The complexes were filtered off and washed with ethanol, ether and then dried over vacuum using $CaCl_2$.

2.4. Biological investigation

2.4.1. Antibacterial activity

Four different bacteria were used in this study to test the activity of eight metal complexes of the two ligands. These were three Gram-positive bacteria: *Bacillus thuringiensis*, *Staphylococcus aureus*, *Streptococcus* sp. and one Gram-negative bacterium: *Pesudomonas aeroginosa*. Their antibacterial activities been assayed using the disk diffusion sensitivity testing method developed by Kirby–Bauer for testing antibiotic sensitivity. In this method the pure bacterial culture (either Gram-positive or Gram-negative) was spread evenly on the surface of LB agar plate and filter paper discs saturated with the either the ligand or any of the complexes were placed onto the surface of the cultivate medium and incubated at 30–37 °C for overnight. Next morning the data were recorded and tabulated.

2.4.2. Antifungal activity

The antifungal activities of the two ligands and their metal complexes were tested against two important fungi isolates; namely *Aspergillus niger* and *Fusarium oxysporium*. Both fungi belong to the Ascomycota and cause serious plant and human diseases. They been assayed using the disc assay (as previously mentioned).

2.5. Molecular modeling

To emphasis on the coordination behavior of the two thiosemicarbazides used towards some heavy metals, some molecular modeling parameters were calculated. The geometry optimization and conformational analysis has been performed by the use of MM^+ force-field as implemented in hyperchem 5.1 [9]

2.6. Equipments

Carbon, H and N were analyzed at the Microanalytical Unit of Cairo University. The metal contents were determined gravimetrically by converting the compounds to their corresponding oxides. The Cl ions were gravimetrically determined using a standard method [10] and the data reflect the high conformity with that theoretically proposed. The molar conductivities of freshly prepared 1.0×10^{-3} mol/cm^3 DMSO solutions were measured for the soluble complexes using Jenway 4010 conductivity meter. The infrared spectra, as KBr discs, were recorded on a Mattson 5000 FTIR Spectrophotometer (400–4000 cm^{-1}) at Mansoura University. The electronic and ^{1}H NMR (200 MHz) spectra were recorded on UV_2 Unicam UV/Vis, and a Varian Gemini Spectrophotometers, respectively at Mansoura and Cairo universities. The thermal studies were carried out on a Shimadzu thermogravimetric analyzer at a heating rate of 10 °C min^{-1} under nitrogen till 1500 °C in King Khaled University, Saudi Arabia. The biological study was carried out in Molecular Biology Center in Botany Department in Mansoura University, Egypt.

3. Results and discussion

The elemental analysis and some physical characteristics are summarized in Table 1. All the isolated complexes are stable in air, having high melting points (over 300 °C), insoluble in H_2O and most organic solvents except DMSO and DMF. They are completely soluble. The molar conductivity measurements for (1.0×10^{-3} mol) in DMSO solvent are found within the non-conducting feature for 1-(2-methoxybenzylidene) thiosemicarbazide complexes but all 1-(naphthalene-2-ylmethylene) thiosemicarbazide complexes are highly conducting. The conductivity feature of MHL^1 complexes belongs to positively charged coordination sphere ionically attached with one conjugated anion in all investigated. This in agreement with the analytical data which suggest the presence of anion covalently or ionically attached with the central metal ions in MHL^1 complexes.

3.1. IR spectral analysis

The infrared spectra and the mode of bonding in the absence of powerful technique such as X-ray crystallography, infrared spectra have proven to be the most suitable technique to give enough information to elucidate the nature of bonding of the ligands to the metal ions. The significant infrared bands of the thiosemicarbazides and their metal complexes are given in Table 2. The observed bands may be classified into those originating from the ligand and those arising from the bonds formed between metal ions and the coordinating sites. IR spectrum of HL^1 ligand shows bands in the range from 2978 to 3371 cm^{-1}, which can be attributed to $\nu_{as}NH_2$, ν_sNH_2 and νCH groups. The bands assigned to νNH and νSH in the free ligand spectrum support the presence of the ligand and in its two tautomer forms (thiole–thione) at the same time. The free ligand showed a strong band at 1642 cm^{-1} for azomethine (CH=N) group [11]. Coordination of HL^1 towards the metals through the nitrogen atom is expected to reduce electron density in the azomethine link and lower the νC=N absorption frequency. The band of νC=N is shifted to lower frequencies and appears around 1612–1624 cm^{-1} due to the coordination of its nitrogen [12]. This coordination is further supported by the appearance of bands in the range of 502–555 cm^{-1} due to νM–N. The ligand coordinates in binuclear complexes with all metal ions by molar ratio 2:2 by two different features. The first feature was done through thione S atom beside the azomethine nitrogen. The second feature is the coordination of another ligand molecule in its thiole form inside the same complex nucleus. Such suggestion is supported by the lower shift in νSH band in all isolated complexes. This proposal was also supported strongly by the data abstracted from ^{1}H NMR beside the former IR data for some complexes. Also the coordination through S atom is supported by the presence of νM–S around to 410–429 cm^{-1} range [13]. The IR spectrum of HL^2 free ligand and its complexes was discussed. A comparison between the complexes spectra with their relative ligand reveals more or less unshift observed in ν_{as}, ν_s, NH_2, νNH, δNH_2, δNH and νCH=N bands. The ν_{IV}C=S band is suffered lower shift in Sb(III) and Pb(II) complexes. As well as, in Sb(III) and Pb(II) complexes, the two ligands molecules are participated by 1M:2HL molar ratio. This is proposed based on elemental analysis and the following IR data: (i) the lower shift observed for ν_{IV}C=S band supports the participation of one ligand in its thione form as well as, the presence of band assigned to νSH supports, the presence of another molecule by its thiole form in the same complex molecule [14]. In addition to slightly modification on account of coordination infrared spectra of the Pb(II) complex show absorption bands at 1297, 766, and 998 cm^{-1} due to coordinated nitrato group. These bends are assigned to ν_1, ν_3 and ν_5 modes, respectively and their frequencies are consistent with those associated with terminally bonded nitrato group [15]. The

Table 2
Assignments of the IR Spectral bands (cm^{-1}) for thiosemicarbazide ligands and their metal complexes.

Compound	$\nu_{OH\ of\ H_2O}$	ν_{asNH_2} ν_sNH_2	$\nu_{C=N}$	ν_{NH}	δ_{NH_2}	δ_{NH}	ν_{SH} $\nu^{I}_{C=S}$	$\nu^{IV}_{C=S}$ $\nu^{II}_{C=S}$	ν_{M-N}	ν_{M-S}
(1) $HL^1[C_{12}H_{11}N_3S]$	–	3371	1642	3173	1616	1532	2369	799	–	–
		3264					1467	1287		
(2) $[Sn_2Cl_3(C_{12}H_{11}N_3S)_2]Cl{\cdot}4H_2O$	3438	3365	1624	3154	1600	1541	2360	797	555	428
		3265					1462	1294		
(3) $[Sb_2Cl_5(C_{12}H_{11}N_3S)_2]Cl{\cdot}4H_2O$	3440	3255	1610	3100	1597	1541	2361	827	550	429
		3145					1461	1294		
(4) $[Pb_2(NO_3)_3(C_{12}H_{11}N_3S)_2](NO_3){\cdot}2H_2O$	3437	3369	1612	3154	1596	1540	2360	796	553	427
		3261					1460	1297		
(5) $[Bi_2Cl_5(C_{12}H_{11}N_3S)_2]Cl{\cdot}2H_2O$	3388	3263	1615	3150	1524	1424	2360	772	502	410
		3166					–	–		
(6) $HL^2[C_9H_{11}N_3SO]$	–	3410	1595	3110	1536	1457	2020	815	–	–
		3293					1367	1239		
(7) $[SnCl_2(C_9H_{11}N_3SO)H_2O]$	3520	3412	1597	–	1540	1462	2031	–	ν_{M-O}	480
		3296					1365	1249	530	
(8) $[SbCl_3(C_9H_{11}N_3SO)_2]H_2O$	–	3415	1596	3166	1540	1480	2362	802	–	480
		3296					1462	1251		
(9) $[Pb(NO_3)(C_9H_{11}N_3SO)_2]$	–	3410	1595	3150	1536	1457	2399	811	ν_{M-O}	480
		3293					1428	1240	560	
(10) $[BiCl_3(C_9H_{11}N_3SO)_2H_2O]H_2O$	3544	3412	1598	–	1545	1478	2361	–	531	475
		3287					1461			

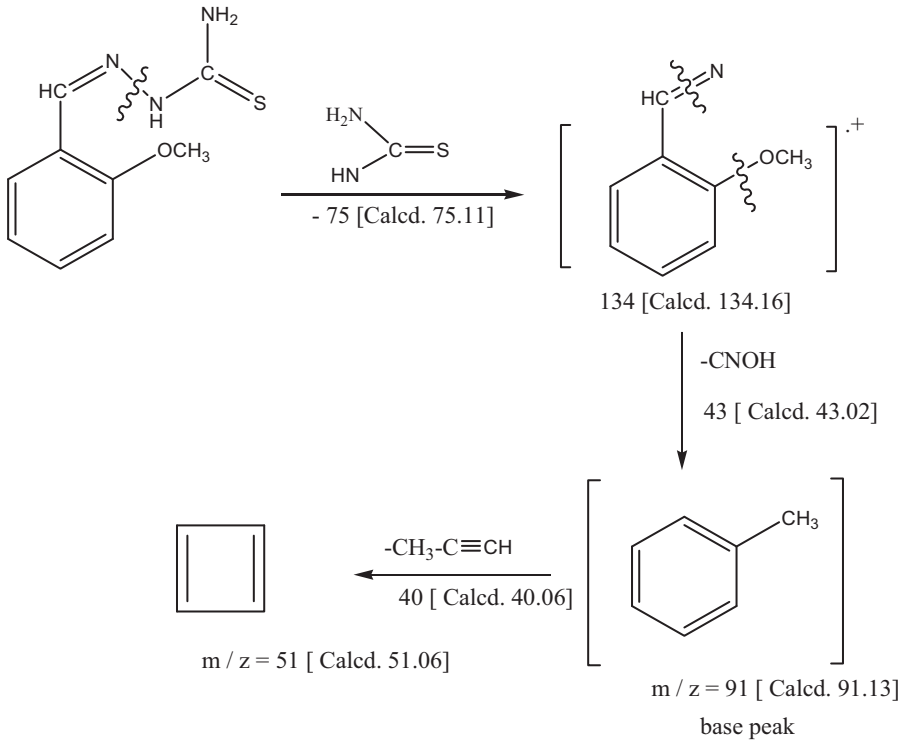

Scheme 1. The fragmentation pattern proposed for 1-(2-methoxybenzylidene) thiosemicarbazide.

shift in νSH band observed in Sn(II) and Bi(III) complexes, supports the participation of the only ligand molecule as thiole form by 1:1 molar ratio. All complexes except Pb(II) one, the νM–Cl band cannot easily detected due to the wave number scanning range ended at $\approx$450 cm^{-1} which don't includes the value of terminal M–Cl band rather than bridging chlorine [16]. The presence of band assigned to νM–S supports the S atom is the only donor atom coordinates from HL^2 ligand.

3.2. Mass spectral analysis

Mass spectrometry has been successfully used to investigate molecular species in solution [17]. The pattern of mass spectrum gives an impression for the successive degradation of the target compound with the series of peaks corresponding to various fragments. Also, the peak intensity gives an idea about the stability of fragments especially with the base peak. The recorded mass spectrum of HL^2 ligand reveals molecular ion peak confirms strongly the proposed formula. The spectrum of the ligand having peak at 209 [25.2% *m*/*z*] which is referring to the molecular ion peak (M^++1) and confirming the purity of the ligand prepared. The degradation patterns have prominent peaks at 134 [38.9% *m*/*z*], 91 [100% *m*/*z*] and 51 [87.4% *m*/*z*] as displayed in degradation Scheme 1.

3.3. ^{1}H NMR spectral analysis

The ^{1}H NMR spectrum of each ligand and some of its related complexes were recorded to confirm the binding mode of two thiosemicarbazides towards the metal ions. The spectrum of HL^1 ligand showed a s, 1H at δ = 11.45 ppm for SH proton, its down field appearance may be due to the participation of SH group in H-bonding with its neighboring, m, 7H at δ = 7.58–8.91 range for aromatic protons, s, 2H at δ = 4.49 for NH_2, peaks at δ = 3.33, 7.48 and 2.51 for H_2O in DMSO, NH in thione form and CH=N + DMSO. The assignment for the spectrum peaks proposed the presence of free ligand in its tautomer forms. The significant peaks appeared in the spectra of Sn(II) and Sb(III) complexes showed singlet peak at δ = 11.45 ppm for SH proton coordinated in its thiole form after the removal of intramolecular H-bonding which may cause unaffected appearance after complexation. S, 1H peak at δ = 9.89 and 8.92 in two complexes supports the down field shift for NH peak found in thione tautomer form inside the binuclear complex. Also, the down field appearance of azomethine protons (δ = 7.54 and 7.58, respectively) in the two complexes supports the participation of its electron donor site (N) in coordination. The other peaks at δ = 3.34 and 3.40 for H_2O in DMSO; 2.512 for DMSO and peaks at δ = 2.09 and 1.92 for NH_2 group which is sided from coordination in the two complexes. The spectrum of HL^2 ligand showed peaks at δ = 11.41, 6.95, 3.82, 3.36 and 2.504 assigned for SH, CH=N, (OCH_3 + H_2O in DMSO), NH_2 and DMSO. As well as, m, 4H at δ = 8.41–6.99 ppm chemical shift assigned for hydrogen of symmetrical aromatic ring ligand. This data abstracted from the spectrum appeared by the same manner in HL^1 as its tautomer appearance. As well as, the presence of interligand H-bonding with its neighboring electronegative atoms (N, O) caused a downfield appearance for SH peak. The spectra of Sn(II) and Sb(III) complexes showed a significant unchangeable appearance in peaks position. The peak appeared at δ = 11.41 ppm assigned for SH in the two complexes spectra may conclude the participation of SH group in coordination as discussed in the two previous complexes. The chemical shift of CH=N group in the two complexes are appeared at δ = 6.96 and 6.95 which reveals its unaffected position. This is reflecting its ruling out from coordination. Also, the other peaks which are completely unaffected as δ = 3.82 for (OCH_3 + H_2O in DMSO) at; δ = 3.35 and 3.63 for NH_2 + H_2O in complexes; δ = 2.5 and 2.51 for DMSO. Such abstracted data supports the proposed mode of coordination based on IR spectra. The two complexes chosen for ^{1}H NMR study (Sn(II) and Sb(II)) are being due to their best solubility in DMSO in comparing with the others under investigation.

Table 3
Electronic spectral bands (nm) of the ligands and their complexes.

Compound	Intraligand and charge transfer (nm)	Proposed geometry
(1) $HL^1[C_{12}H_{11}N_3S]$	276, 318, 364, 378	–
(2) $[Sn_2Cl_3(C_{12}H_{11}N_3S)_2]Cl{\cdot}4H_2O$	276, 318, 355, 388	Tetrahedral
(3) $[Sb_2Cl_5(C_{12}H_{11}N_3S)_2]Cl{\cdot}4H_2O$	276, 318, 355, 370, 452	Trigonal bipyramidal
(4) $[Pb_2(NO_3)_3(C_{12}H_{11}N_3S)_2](NO_3){\cdot}2H_2O$	276, 318, 354, 370	Tetrahedral
(5) $[Bi_2Cl_5(C_{12}H_{11}N_3S)_2]Cl{\cdot}2H_2O$	276, 318, 356, 360, 452	Trigonal bipyramidal
(6) $HL^2[C_9H_{11}N_3SO]$	274, 300, 364	–
(7) $[SnCl_2(C_9H_{11}N_3SO)H_2O]$	270, 308, 364, 380, 475	Tetrahedral
(8) $[SbCl_3(C_9H_{11}N_3SO)_2]H_2O$	274, 296, 316, 364, 425	Trigonal bipyramidal
(9) $[Pb(NO_3)(C_9H_{11}N_3SO)_2]$	270, 308, 356	Tetrahedral
(10) $[BiCl_3(C_9H_{11}N_3SO)H_2O]H_2O$	274, 296, 316, 364, 425	Trigonal bipyramidal

3.4. Electronic spectral analysis

The spectral data of the free ligands and their complexes in DMSO are listed in Table 3. The electronic spectra of free ligands showed two types of transitions, the first type appeared at the range 274–318 nm which can be assigned to $\pi \rightarrow \pi^*$ transition due to transition involving molecular orbital located in the aromatic ring. These peaks have been relatively unaffected in the spectra of the complexes; this is expected for the relatively nil role of aromatic ring in complexation [18]. The second type of transitions appeared at range 300–378 nm, which can be assigned to $n \rightarrow \pi^*$ transition due to involving molecular orbitals of the C=N chromophore. The bands of $n \rightarrow \pi^*$ transition have been shifted upon complexation of 1-(naphthalene-2-ylmethylene) thiosemicarbazide ligand towards all metal ions. This is indicating that, the azomethine group nitrogen atom appears to be coordinated to the metal ions [19]. However, this observation is not appeared in 1-(2-metoxybenzylidene) thiosemicarbazide complexes spectra which may give a hint for excluding CH=N group from coordination. The spectra of some complexes show other bands did not appear in the free ligands. The spectra of Bi(III) and Sb(III)–HL^1 complexes reveal a new band at 452 nm as well as Sn(II), Sb(III) and Bi(III)–HL^2 complexes reveal new bands at 475, 425 and 425 nm. These additive bands assigned to ligand to metal charge transfer. Such appearance are considered a significant and pointed to the possibility of these bands for spectrophotometric determination for such metal ions. The spectrophotometric determination of these metals is analytically essential especially with the use of simple economic procedure. The structural formula of all isolated complexes (Figs. 2 and 3) was proposed based on the nature of electronic configuration of metal ions without any other concepts, as the tetrahedral geometry was proposed for Sn(II) and Pb(II) complexes but the trigonal bipyramidal is the other geometry proposed for higher oxidation state metal ions (Sb(III) and Bi(III)) complexes.

3.5. Phenomenological aspects of thermal analysis

The phenomenological aspects of the present complexes are tabulated in Table 4. The HL^1 ligand it undergoes three stages of decomposition in the range 213–690 °C. The first stage starts at 213 °C by an observable mass loss 69.20% may be attributed to the decomposition of $C_4H_7N_3OS$ moiety. The second stage started at 337 °C by a mass loss 12.32% may be attributed for C_2H_2 decomposition. The third stage started at 587 °C by an observable weight loss 17.78% may refer to the removal of remaining part of the ligand (C_7H_5N). The Sn(II) complex TG curve, displays fifth degra-

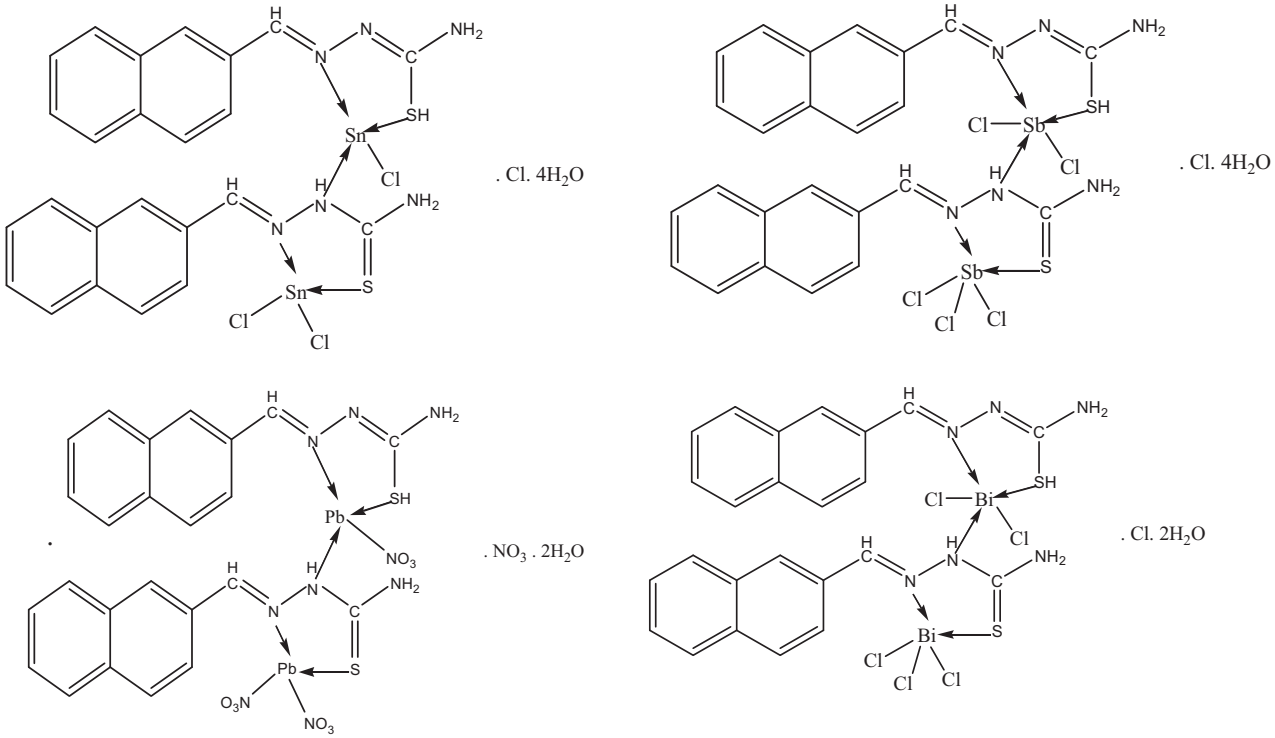

Fig. 2. The structural formulas proposed for HL^1 complexes.

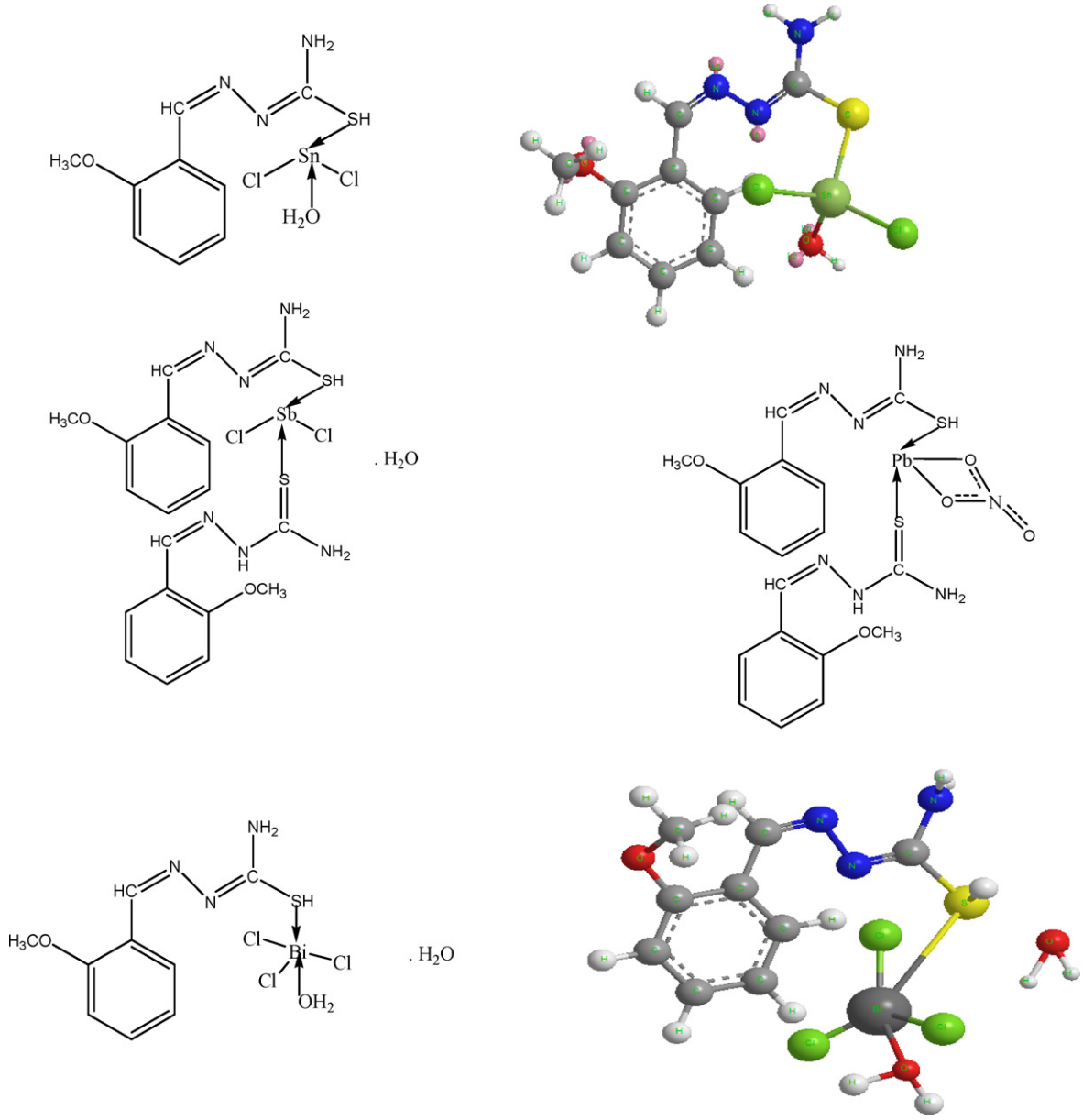

Fig. 3. The structural formulas proposed for HL^2 complexes.

dation stages in the temperature range 50–780 °C. The first stage started at 50 °C by an observable mass loss 8.10% is attributing to the removal of hydrated water molecules. The second stage started at 100 °C by an observable mass loss 11.62% may be attributed to the decomposition of $1.5Cl_2$ molecules. The third stage started at 220 °C by an observable mass loss by 3.92% may be attributed to the decomposition of $0.5Cl_2$. The fourth stage started at 370 °C by an observable mass loss 20.52% may be attributed to the decomposition of $C_{11}H_{11}N_3$ organic moiety. The fifth degradation stage started at 530 °C by an observable mass loss 20.41% may be attributed to the decomposition of $C_{11}H_{11}N_3$. The final residue suggested as 2SnS + 2C by an observable mass 28.32%. The TG curve of Sb(III) complex displays four decomposition stages in the temperature range 60–760 °C. The first stage starts decomposition at 60 °C by an observable mass loss 7.1% attributed to the loss of hydrated water molecules. The second stage starts decomposition at 120 °C by an observable mass loss 14.22% may be attributed to the removal of $2Cl_2$. The third stage starts decomposition at 240 °C by an observable mass loss 25.81% may be attributed to the removal of $Cl_2 + C_{11}H_{11}N_3$. The fourth stage starts decomposition at 500 °C by an observable mass loss 22.1% may be attributed to the removal of $C_{11}H_{11}N_3$. The residual part by an observable weight percentage 30.77% may be considered to SbS + Sb + 2C. The TG curve of the thermal decomposition of Pb(II) complex displays four degradation stages in the temperature range 60–750 °C. The first decomposition stage starts at 60 °C by an observable mass loss 2.95% is attributed to the decomposition of hydrated water molecules. The second decomposition stage starts at 150 °C by an observable mass loss 21.25% may be attributed to the removal of $4NO_2 + 2O_2$. The third decomposition stage starts at 260 °C by an observable mass loss 15.91% may be attributed to the removal of $C_{11}H_{11}N_3$. The fourth decomposition stage starts at 500 °C by an observable mass loss 15.90% may be attributed to the removal of $C_{11}H_{11}N_3$. The residual part by an observable weight percentage 43.98 is attributed to 2PbS + 2C. The TG curve of Bi(III) complex displays fifth degradation stages in the temperature range 50–780 °C.

Table 4
Thermogravimetric data of the investigated ligands and their complexes.

Complex	Steps	Temp. range (°C)	Decomposed assignments	Weight loss Found (Calcd. %)
(1)	1st	180–260	$-N_2+H_2+CS$	32.41 (32.32)
	2nd	260–310	$-C_4H_4$	22.92 (22.71)
	3rd	310–420	$-C_7H_5N$	44.67 (44.97)
(2)	1st	50–100	$-4H_2O$	8.10 (7.92)
	2nd	100–220	$-1.5Cl_2$	11.62 (11.69)
	3rd	220–370	$-0.5Cl_2$	3.92 (3.89)
	4th	370–530	$-C_{11}H_{11}N_3$	20.52 (20.36)
	5th	530–780	$-C_{11}H_{11}N_3$	20.41 (20.36)
	Residue		2SnS + 2C	35.43 (35.78)
(3)	1st	60–120	$-4H_2O$	7.10 (7.30)
	2nd	120–240	$-2Cl_2$	14.22 (14.37)
	3rd	240–500	$-Cl_2 + C_{11}H_{11}N_3$	25.81 (25.95)
	4th	500–760	$-C_{11}H_{11}N_3S$	22.10 (22.02)
	Residue		SbS + Sb + 2C	30.77 (30.35)
(4)	1st	60–150	$-2H_2O$	2.95 (3.11)
	2nd	150–260	$-4NO_2 + 2O_2$	21.25 (21.44)
	3rd	260–500	$-C_{11}H_{11}N_3$	15.91 (16.01)
	4th	500–750	$-C_{11}H_{11}N_3$	15.91 (16.01)
	Residue		2PbS + 2C	43.98 (43.43)
(5)	1st	50–150	$-2H_2O$	3.10 (3.20)
	2nd	150–250	$-2Cl_2$	12.55 (12.60)
	3rd	250–440	$-Cl_2$	6.26 (6.30)
	4th	440–650	$-C_{11}H_{11}N_3$	16.41 (16.46)
	5th	650–780	$-C_{11}H_{11}N_3$	16.23 (16.46)
	Residue		2BiS + 2C	45.45 (44.97)
(6)	1st	213–337	$-C_4H_7N_3OS$	69.20 (69.03)
	2nd	337–587	$-C_2H_2$	12.32 (12.44)
	3rd	587–690	$-C_3H_2$	17.78 (18.18)
	Residue			
(7)	1st	100–219	$-H_2O$	4.44 (4.32)
	2nd	219–311	$-Cl_2 + H_2 + 0.5N_2$	20.80 (20.85)
	3rd	311–522	$-C_3H_5N_2S$	24.33 (24.26)
	4th	522–750	$-C_6H_4O$	22.11 (22.09)
	Residue		Sn	28.32 (28.47)
(8)	1st	90–200	$-H_2O$	2.53 (2.71)
	2nd	200–331	$-L + 1.5Cl_2 + SCNH_2$	56.43 (56.53)
	3rd	331–579	$-C_6H_4-OCH_3$	16.26 (16.12)
	4th residue	579–750	$Sb + N_2 + H_2 + C$	24.78 (24.19)
(9)	1st	200–238	$-NO_3 + 1.5N_2 + 2H_2 + C$	17.41 (17.46)
	2nd	238–274	$-N_3C_2H_7O$	12.37 (12.95)
	3rd	274–490	$-C_6H_4-OCH_3$	15.79 (15.58)
	4th	490–538	$-C_6H_4$	11.58 (11.06)
	5th	538–750	PbS + S + 2C	42.84 (42.94)
	Residue			
(10)	1st	34–100	$-H_2O$	3.73 (3.21)
	2nd	100–281	$-H_2O + 0.5N_2 + H_2$	6.15 (6.07)
	3rd	281–525	$-1.5Cl_2 + C_9H_9N_2OS$	53.22 (53.44)
	4th residue	525–750	–Bi	36.90 (37.27)

The first degradation stage starts at 50 °C by an observable mass loss 3.1% strictly attributed to the removal of hydrated water molecules. The second stage starts at 150 °C by an observable mass loss 12.55% may be attributed to the removal of $2Cl_2$. The third degradation stage starts at 260 °C by an observable mass loss 6.26% may be attributed to the removal of Cl_2. The fourth degradation stage starts at 440 °C by an observable mass loss 16.41% may be attributed to the decomposition of $C_{11}H_{11}N_3$ organic moiety. The fifth degradation stage starts at 650 °C by an observable mass loss 16.23% may be attributed to the decomposition $C_{11}H_{11}N_3$. The residual part by a weight percentage 45.45% may be for 2BiS + 2C. The HL^2 ligand undergoes three stages of decomposition in the range 213–690 °C. The first stage starts at 213 °C by an observable mass loss 69.2% may be attributed to the decomposition of $C_4H_7N_3OS$ organic moiety. The second stage starts at 337 °C by an observable mass loss 12.32% may be attributed to the decomposition of C_2H_2. The final stage starts at 587 °C by an observable mass loss 17.78% may be attributed to the removal of remaining organic part (C_3H_2). The TG curve of Sn (II) complex displays four degradation stages in the temperature range 100–750 °C. The first stage starts decomposition at 100 °C by an observable mass loss 4.44% is attributed to the removal of coordinated water molecule. The second decomposition stage starts at 219 °C by an observable mass loss 20.80% may be attributed to the removal of $Cl_2 + H_2 + 0.5\,N_2$. The third degradation stage starts at 311 °C by an observable mass loss 24.33% may be attributed to the removal $C_3H_5N_2S$ organic moiety. The fourth stage starts at 522 °C by an observable mass loss 32.11% may be attributed to the removal of C_6H_4O. The residual part by an observable weight percentage 28.32 may be attributed to Sn. The TG curve of Sb(III) complex displays three degradation stages in the temperature range 90–750 °C. The first stage starts at 90 °C by an observable mass loss 2.53% is attributed to the removal of hydrated water

Table 5
Theoretical data implementing molecular modeling for the two free ligands.

The assignment of the theoretical parameters	The compound investigated	The theoretical data
Total energy	(1) Thione form of HL[1]	−52,096.8553413 (kcal/mol)
Total energy		−83.021613313 (a.u.)
Binding energy		−2864.8719423 (kcal/mol)
Isolated atomic energy		−49,231.9833990 (kcal/mol)
Electronic energy		−323,909.9016138 (kcal/mol)
Core–core interaction		271,813.0462726 (kcal/mol)
Heat of formation		164.3300577 (kcal/mol)
Dipole moment		7.238 (Debyes)
HOMO		−8.738
LUMO		−1.146
Total energy	(2) Thiol form of HL[1]	−52,092.9364237 (kcal/mol)
Total energy		−83.015368121 (a.u.)
Binding energy		−2860.9530247 (kcal/mol)
Isolated atomic energy		−49,231.9833990 (kcal/mol)
Electronic energy		−321,511.0667514 (kcal/mol)
Core–core interaction		269,418.1303278 (kcal/mol)
Heat of formation		168.2489753 (kcal/mol)
Dipole moment		4.113 (Debyes)
HOMO		−8.708
LUMO		−0.905
Total energy	(3) Thione form of HL[2]	−50,705.7212863 (kcal/mol)
Total energy		−80.804700357 (a.u.)
Binding energy		−2496.4471153 (kcal/mol)
Isolated atomic energy		−48,209.2741710 (kcal/mol)
Electronic energy		−288,950.8906111 (kcal/mol)
Core–core interaction		238,245.1693249 (kcal/mol)
Heat of formation		79.6438847 (kcal/mol)
Dipole moment		10.297 (Debyes)
HOMO		−8.668
LUMO		−0.890
Total energy	(4) Thiol form of HL[2]	−50,709.7766309 (kcal/mol)
Total energy		−80.811162959 (a.u.)
Binding energy		−2500.5024599 (kcal/mol)
Isolated atomic energy		−48,209.2741710 (kcal/mol)
Electronic energy		−287,011.5101966 (kcal/mol)
Core–core interaction		236,301.7335657 (kcal/mol)
Heat of formation		75.5885401 (kcal/mol)
Dipole moment		(Debyes) 3.582
HOMO		−8.775
LUMO		−0.608

molecule. The second stage starts at 200 °C by an observable mass loss 56.03% may be attributed to the removal of HL + $1.5Cl_2$ + $SCNH_2$. The third stage starts at 331 °C by an observable mass loss 16.66% may be attributed to the removal of $C_6H_4OCH_3$. The residual part by a weight percentage 24.78 may be attributed to Sn + N_2 + H_2 + C. The TG curve of Pb(II) complex displays fifth degradation stages in the temperature range 200–750 °C. The first stage starts at 200 °C by an observable mass loss 17.41% may be attributed to the decomposition of NO_3 + 1.5 N_2 + $2H_2$ + C. The second degradation stage starts at 238 °C by an observable mass loss 12.37% may be attributed to removal of $C_2H_7N_3O$ organic moiety. The third stage starts at 274 °C by an observable mass loss 15.79% may be attributed to the removal of $C_6H_4OCH_3$. The fourth stage starts at 490 °C by an observable mass loss 11.58% may be attributed to the removal of C_6H_4. The residual part by a weight percentage 42.84 may be attributed to PbS + S + 2C. The TG curve of Bi(III) complex reveals four degradation stages in the temperature range 34–750 °C. The first stage starts at 34 °C by an observable mass loss 3.73% is attributed to the removal of hydrated water molecule. The second stage starts at 100 °C by an observable mass loss 6.35% may be attributed to the removal of H_2O + 0.5 N_2 + H_2. The third stage starts at 281 °C by an observable mass loss 53.02% may be attributed to the removal of $1.5Cl_2$ + $C_9H_9N_2OS$. The final stage starts at 525 °C by an observable mass 36.9% may be attributed to Bi. The TG analysis aspect

Table 6
Antibacterial antifungal data of the ligands and their metal complexes.

Fusarium oxysporium	*Aspergillus niger*	*Pesudomonas aeroginosa*	*Streptococcus* sp.	*Staphylococcus aureus*	*Bacillus thuringiensis*	Compound
++	++	+++	+++	+++	+++	(1)
+++	+++	++++	+++	+++	++	(2)
++	+++	++++	+++	+++	++++	(3)
+++	++	++++	+++	++	++	(4)
+++	++	++++	++++	++++	++	(5)
+++	++	+++	++	+++	+	(6)
+++	++	++	++++	++++	+++	(7)
+++	+++	++	+++	+++	++++	(8)
++	+++	++++	+++	+++	++++	(9)
+++	+++	+++	++	++++	++++	(10)

(++++) good activity (90–100% inhibition); (+++) moderate activity (75–85% inhibition); (++) significant activity (50–60% inhibition).

of the free ligands may reflect their thermal stability. The trend of their thermal decomposition in the free state may be pointed to their decomposition behavior inside the investigated complexes. Also, the higher conformity in between the observed and calculated mass loss is the main feature for the degradation proposed in all complexes. The presence of residual (metal sulphide or free metal) polluted with other organic atoms may be due to the recording of residual part at a relatively lower temperature. I think if the degradation completed up to 1000 °C all the polluted atoms will be expelled completely.

3.6. Molecular modeling

The MM^+ force-field implemented in hyperchem 5.1 (Table 5), was applied on the free ligands only. This is used as a further conformity tool for the presence of thiosemicarbazide ligands in their tautomer forms (thione–thiol). The spectral data (IR and ^1H NMR) abstracted for the two ligands in their free state suggests strongly their presence in thiol–thione forms. The theoretical data of the molecular modeling (total energy, binding energy, isolated atomic energy, electronic energy, heat of formation, dipole moment, HOMO and LUMO) implementing the hyperchem program especially with, total energy, binding energy, isolated atomic energy, electronic energy and heat of formation values reflect the stability of thiole form in comparing with its thione by a small difference in the two ligands. This is supporting the proposal of their presence suggested with the complexes isolated.

3.7. Antibacterial and antifungal studies

The biological activity of the two ligands and their metal complexes were tested by paper disc diffusion method against diversity of bacteria and fungi because of these microorganisms can get resistance to antibiotics and their metal complexes through biochemical and morphological modifications [20], %RSD was calculated to investigate significant differences in the three repeated results. Antibacterial activity of all complexes at low concentrations is quite significant and increases with increasing concentrations. The results of the antibacterial study of the synthesized compounds are displayed in Table 6. The results were expressed as; excellent activity (150–200% inhibition), good activity (90–100% inhibition) moderate activity (75–85% inhibition), significant activity (50–60% inhibition), negligible activity (20–30% inhibition). Ligand HL^1 shows moderate activity against both types of bacteria. While some of its complexes have a good activity against Gram positive and Gram negative organisms. The HL^2 ligand shows somewhat moderate activity against two bacteria types. However, some of its complexes reveal a good activity towards Gram-positive and Gram-negative organisms. All the ligands and their complexes reveal a moderate to significant activity in antifungal studies. The enhanced intrinsic activity of complexes can be explained on the basis of cell permeability, the lipid membrane around the cell favors the penetration of lipid-soluble materials, and liposolubility is an important factor that controls the antimicrobial activity. On chelation the polarity of the metal ions will be reduced due to the overlap of ligand orbitals and partial sharing of the positive charge of the metal ion with donor groups [21]. It is likely that the increased liposolubility of the ligand upon metal complexation may contribute to its facile transport into the bacterial cell which blocks the metal binding sites in enzymes of microorganisms [22]. The complexes have a relative best activity as compared to their ligands towards the fungi (Table 6). It is suggested that the antifungal activity of the complexes is due to either by killing the microbes or inhibiting their multiplication by blocking their active sites through the interaction of metalloprotein enzyme active sites with the central metal ions in the complexes.

References

[1] S.N. Pandeya, J.R. Dimmock, Pharmazie 48 (1993) 659.
[2] M. Akbar Ali, S.E. Livingstone, Metal complexes of sulphur-nitrogen chelating agents, Coord. Chem. Rev. 13 (2–3) (1974) 101–132.
[3] D.W. West, S.B. Padhye, P.B. Sonawane, Structure and physical correlations in the biological properties of the transition metal hetero cyclic thiosemicarbazines and S-alkyl dithiocarbonate complexes Structure and Bonding, 76, Springer, Berlin, 1991, p. 1–49.
[4] A.K. El-Sawaf, D.X. West, R.M. El-Bahnasawy, F.A. El-Saied, Transit. Met. Chem. 23 (1998) 227.
[5] M. Joseph, M. Kuriakose, M.R.P. Kurup, E. Suresh, A. Kishore, S.G. Bhat, Polyhedron 25 (2006) 612.
[6] F.M. Belicchi, F. Bisceglie, G. Pelosi, J. Inorg. Biochem. 83 (2001) 169.
[7] S.K. Chawla, S. Kaur, N. Gupta, G. Hundal, Endleev Commun. 17 (6) (2007) 335.
[8] N. Kumar, A. Saxena, B. Tiwari, M. Agarwal, N. Pal, J.N. Gurtu, R. Gupta, Bull. Pure Appl. Sci.: Chem. (2006).
[9] Hyper Chem, Version 7.51 Hyper Cube, Inc.
[10] A.I. Vogel, A Text Book of Quantitative Inorganic Analysis, Longmans, London, 1994.
[11] R. Ramesh, S. Maheshwaram, J. Inorg. Biochem. 96 (2003) 457.
[12] S.A. Ali, A.A. Soliman, M.M. Aboaly, R.M. Ramadan, J. Coord. Chem. 55 (2002) 1161.
[13] P. Souza, F. Kaiser, J.R. Moguer, A. Arquero, Transit. Met. Chem. 12 (1987) 128.
[14] N.M. El-Metwally, A.A. El-Asmy, Coord. Chem. 59 (2006) 1591.
[15] (a) C.C. Addision, D. Sultons, Prog. Inorg. Chem. 8 (1967) 195;
(b) C.C. Addision, N. Logan, S.C. Wall Work, C.D. Garner, Quart. Rev. Chem. Soc. 25 (1971) 289.
[16] K. Nakamoto, Infrared and Raman Spectra of Inorganic and Coordination Compounds, Wiley, New York, 1978.
[17] (a) J. Sanmartin, F. Novio, A.M. Garcia-Deibe, M. Fondo, N. Ocampo, M.R. Bermejo, Polyhedron 25 (2006) 1714;
(b) I. Beloso, J. Castro, J.A. Garcia-Vazquez, P. Perez-Lourido, J. Romero, A. Sousa, Polyhedron 22 (2003) 1099.
[18] R.K. Sharma, R.V. Singh, J.P. Tandon, J. Inorg. Nucl. Chem. 42 (1980) 1382.
[19] M.J.M. Cambell, Coord. Chem. Rev. 15 (1975) 279.
[20] W. Rchman, M.K. Baloch, A. Badshah, Eur. J. Med. Chem. 43 (2008) 2380.
[21] H. Koksal, M.K. Sener, Transit. Met. Chem. 24 (1999) 414.
[22] I. Muhammad, I. Javed, I. Shahid, I. Nazia, Turk. J. Biol. 31 (2007) 339.